SOME CLEO RESULTS ON B AND CHARM PHYSICS

GIANCARLO MONETI
Department of Physics, Syracuse University, Syracuse, NY, 13244, U.S.A.
On behalf of the CLEO Collaboration

Abstract

I briefly summarize the results of nine recent analyses, out of the twentytwo papers that the CLEO Collaboration sent for publication since after the year 2000 Summer conferences. They are, on B Physics: the observation of $B \rightarrow \phi K$ and $B \rightarrow \phi K^*$, a new limit on $\mathcal{B}(B \rightarrow \pi^\circ \pi^\circ)$, the γ energy spectrum and branching ratio for the $(b \rightarrow s\gamma)$ process and an improved method of extracting CP asymmetry from $B\overline{B} \rightarrow \ell^\pm \ell^\pm$. On Charm Physics and fragmentation: some new results on D° mixing, CP violation and Doubly Cabibbo Suppressed Decays (DCSD), the first measurement of the $D^{*\pm}$ width, $\Gamma(D^{*+})$, and some unexpected $\Lambda_c \overline{\Lambda}_c$ correlations in $e^+e^- \rightarrow c\overline{c}$. I'll also list the references to the thirteen topics that I omited.

1 The Data

The results I'll show come from the analysis of 13.8 fb^{-1} of data collected, with the CLEO II [1] and CLEO II.V [2] detectors, at the Cornell Electronpositron Storage Ring, CESR, between Nov. 1990 to Feb. 1999, running at the peak of the $\Upsilon(4S)$ resonance and just below the threshold for $B\overline{B}$ production. That means about 9.74 M $e^+e^- \to B\overline{B}$ at the $\Upsilon(4S)$, 16.8 M $e^+e^- \to c\overline{c}$ events (plus charm from B decays) and 12.6 M $e^+e^- \to \tau^+\tau^-$ events. The CLEO II.V detector is showm in fig.1.
I remind you that CLEO has, besides good tracking and particle ID from ionization and time of flight, an excellent E.M. shower detector and good hermiticity.

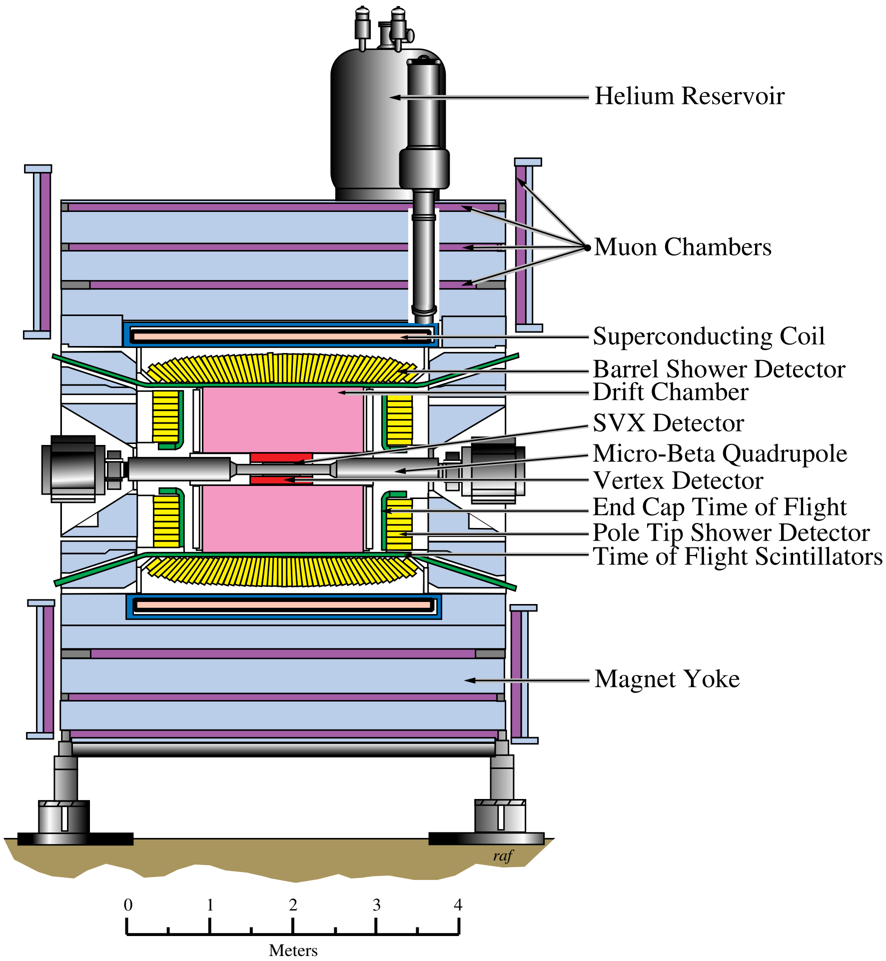

Figure 1: Schematic of the CLEO II.V detector at CESR

2 B Physics

I'll briefly summarize very recent results on four topics:

- Observation of $B \to \phi K$ and $B \to \phi K^*$ and first measurement of the respective branching ratios [3].
- New limit on $\mathcal{B}(B \to \pi^\circ \pi^\circ)$ [4].
- $b \to s\gamma$, hadronic mass moments in $B \to X_c \ell \nu$, V_{cb} and V_{ub} [5].
- Limit on CP asymmetry in $B^\circ \overline{B}^\circ \to \ell^\pm \ell^\pm$ [6].

3 The $B \to \phi K$ and $B \to \phi K^*$ decays [3]

The decays $B \to \phi K$ and $B \to \phi K^*$ are a clear signature for gluonic penguin processes (fig. 2). They can be used to measure the $\sin 2\beta$ parameter of the Unitarity Triangle.

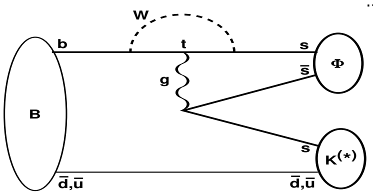

Figure 2: Penguin diagram describing $B \to \phi K^{(*)}$ decays

We used the following topologies: ϕK^-, ϕK°_S, ϕK^*, with $\phi \to K^+ K^-$, $K^* \to (K^- \pi^+, K^\circ_S \pi^\circ, K^- \pi^\circ, K^\circ_S \pi^-)$ and $K^\circ_S \to \pi^+ \pi^-$.

In these decay channels the $B\overline{B}$ and non-resonant $K\pi$ backgrounds are found to be negligible. The continuum annihilation background was suppressed via a selection on the Fox-Wolfram parameters: $H_2/H_0 < 0.6$.

The signals were obtained by unbinned Maximum Likelihood fits, performed separately for each topology, using the following variables:
the beam-constrained candidate B mass,
$M_B \equiv \sqrt{E_{beam}^2 - p_B^2}$,
the energy difference, $\Delta E = E_\phi + E_{K(*)} - E_{beam}$,
$p_B \cdot beam$, (thrust of the B candidate)$\cdot$(thrust of remainder), M_ϕ and, when applicable,
the helicity angles, M_{K^*}, and dE/dx information.

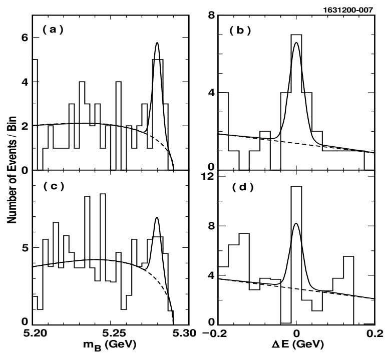

Figure 3: M_B, ΔE plots for (a,b) $B^- \to \phi K^-$, and (c,d) $B^0 \to \phi K^{*0}$

Figure 3 shows the plot of M_B after selection on the ΔE signal region and viceversa, for the ϕK^- (a,b) and ϕK°_S (c,d) channels, with the fitted curves superimposed. The results of the fits are shown in Table1.

Table 1: Intermediate fitted branching fractions ($\mathcal{B}_{fit}$), final branching fraction results ($\mathcal{B}$), and theoretical estimate [7] are given in units of 10^{-6}. When the result is not statistically significant, the final result is quoted as a 90% C.L. upper limit. The errors on branching fractions are statistical and systematic respectively. Reconstruction efficiency $\mathcal{E}$ does not include branching fractions, and it is quoted for modes with K^0 assuming $K^0 \to K^0_S \to \pi^+\pi^-$ decay.

Mode	Yield	$\mathcal{E}$(%)	$\mathcal{B}_{fit}$ $\times 10^6$	Statist. Signif.	$\mathcal{B}$ $\times 10^6$	Theor. $\mathcal{B}$ $\times 10^6$
ϕK^-	$14.2^{+5.5}_{-4.5}$	54	$5.5^{+2.1}_{-1.8} \pm 0.6$	5.4σ	see $\mathcal{B}_{fit}$	0.7-16
ϕK^0	$4.2^{+2.9}_{-2.1}$	48	$5.4^{+3.7}_{-2.7} \pm 0.7$	2.9σ	< 12.3	0.7-13
ϕK comb.	—	—	—	6.1σ	$5.5^{+1.8}_{-1.5} \pm 0.7$	
ϕK^{*0} $(K^-\pi^+)$	$12.1^{+5.3}_{-4.3}$	38	$9.9^{+4.3+1.6}_{-3.5-1.6}$	4.5σ	—	
ϕK^{*0} $(K^0\pi^0)$	$5.1^{+3.9}_{-2.8}$	20	$46.3^{+35.7+5.9}_{-26.0-6.6}$	2.7σ	—	
ϕK^{*0}	—	—	$11.5^{+4.5+1.8}_{-3.7-1.7}$	5.1σ	see $\mathcal{B}_{fit}$	0.2-31
ϕK^{*-} $(K^-\pi^0)$	$3.8^{+4.1}_{-2.8}$	25	$9.3^{+10.1+1.7}_{-7.0\ -1.5}$	1.5σ	—	
ϕK^{*-} $(K^0\pi^-)$	$4.0^{+3.1}_{-2.2}$	32	$11.4^{+9.0+1.8}_{-6.3-1.8}$	2.7σ	—	
ϕK^{*-}	—	—	$10.6^{+6.4+1.8}_{-4.9-1.6}$	3.1σ	< 22.5	0.2-31
ϕK^* comb.	—	—	—	5.9σ	$11.2^{+3.6+1.8}_{-3.1-1.7}$	

One can see that we have measured for the first time $\mathcal{B}(B^- \to \phi K^-) = (5.5^{+2.1}_{-1.8} \pm 0.6) \times 10^{-6}$ and $\mathcal{B}(B^0 \to \phi K^{*0}) = (11.5^{+4.5+1.8}_{-3.7-1.7}) \times 10^{-6}$ each with statistical significance above 5σ.
For the other two decay channels we obtained the following branching fractions: $\mathcal{B}(B^0 \to \phi K^0) = (5.4\,^{+3.7}_{-2.7} \pm 0.7) \times 10^{-6}$ and $\mathcal{B}(B^- \to \phi K^{*-}) = (10.6^{+6.4+1.8}_{-4.9-1.6}) \times 10^{-6}$. Since the statistical significance in these modes is limited we set the following upper limits: $\mathcal{B}(B^0 \to \phi K^0) < 12.3 \times 10^{-6}$ and $\mathcal{B}(B^- \to \phi K^{*-}) < 22.5 \times 10^{-6}$ (at 90% C.L.). Averaging over B^0 and B^- we obtain $\mathcal{B}(B \to \phi K) = (5.5^{+1.8}_{-1.5} \pm 0.7) \times 10^{-6}$ (6.1σ) and $\mathcal{B}(B \to \phi K^*) = (11.2^{+3.6+1.8}_{-3.1-1.7}) \times 10^{-6}$ (5.9σ).
The measured branching fractions lie within the range of theoretical predictions (see Table 1). Since there is considerable spread in these calculations, our results will help constrain model parameters.

4 A new limit on $\mathcal{B}(B^o \to \pi^\circ\pi^\circ)$ [4]

The CP asymmetry in $B \to \pi^+\pi^-$ gives the sum $(\beta + \gamma)$ of phases of the V^*_{td} and V^*_{ub} elements of the CKM matrix, provided that we combine it with $\mathcal{B}(B^+ \to \pi^+\pi^\circ)$ and

$\mathcal{B}(B^o \to \pi^\circ\pi^\circ)$ in an isospin analysis that gives the relative phase of tree and penguin contributions [8].

The $B^\circ \to \pi^\circ\pi^\circ$ has not been observed yet, but we produced a new stringent upper limit on $\mathcal{B}(B^o \to \pi^\circ\pi^\circ)$.

Fig. 4 shows the distribution of event candidates in the usual M_B vs ΔE plot, its projections on the two axes with the selections shown, and the distribution of the *Fisher Discriminant* (event shape) that should help in suppressing continuum annihilation events. The $B^\pm \to \rho^\pm\pi^o$ background is well separated by the ΔE selection.

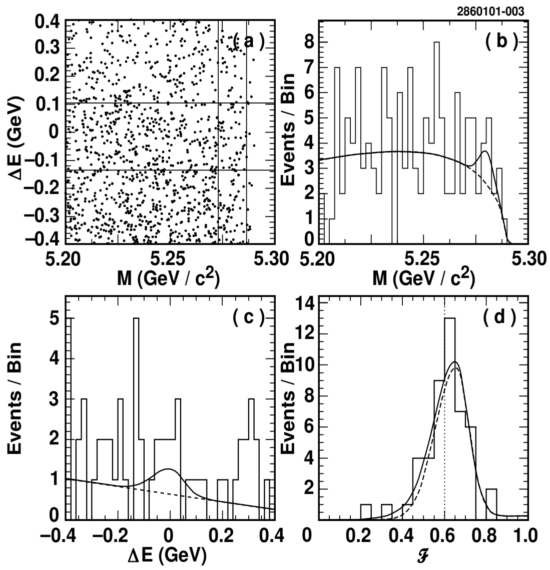

Figure 4: M_B vs ΔE, its projections and the *Fisher Discriminant.*

The unbinned maximum likelihood fit, using M_B, ΔE and the *Fisher Discriminant* finds $N_S = 6.2^{+4.8}_{-3.7}$ (only 2σ significance!) that gives:
$\mathcal{B}(B^o \to \pi^\circ\pi^\circ) = (2.2^{+1.7}_{-1.3} \pm 0.7) \times 10^{-6}$. A series of Monte Carlo simulated experiments give the following 90% confidence level limit:

$$\mathcal{B}(B^o \to \pi^\circ\pi^\circ) < 5.7 \times 10^{-6} \text{ (PRELIMINARY)}. \tag{1}$$

5 $b \to s\gamma$, hadronic mass moments in $B \to X_c \ell \nu$, V_{cb} and V_{ub} [5]

The $b \to s\gamma$ process is a pure electroweak penguin transition (Fig. 5). Its branching ratio is sensitive to the $V^*_{ts}V_{tb}$ product and also to "New Physics" because of new particles forming the loop. It could also be affected by anomalous WWγ coupling.

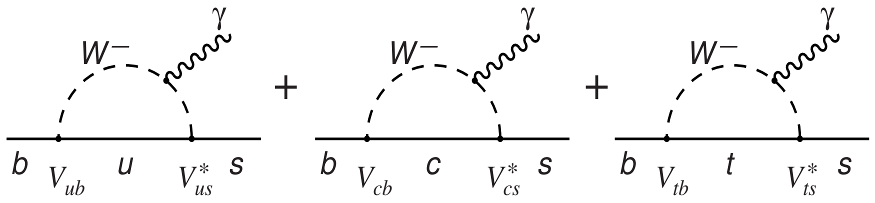

Figure 5: The three penguin diagram of the $b \to s\gamma$ process.

Furthermore, as we'll see below, the moments of the γ spectrum are instrumental for extracting a more precise values of $|V_{ub}|$ and $|V_{cb}|$ from B semileptonic decays. The Standard Model (SM) expectation is for a tiny $\mathcal{B}(B \to X_s \gamma) = (3.3 \pm 0.3) \times 10^{-4}$. The characteristic signature of this process is a somewhat narrow peak of the photon energy spectrum around 2.4 GeV, a region hardly reached by photons from other B decays. The challenge, however, is to extract the tiny $B \to X_s \gamma$ signal from the huge backgrounds of γ from π° and η produced in continuum annihilation and initial state radiation in e^+e^- annihilation, as shown in fig. 6 (log scale).

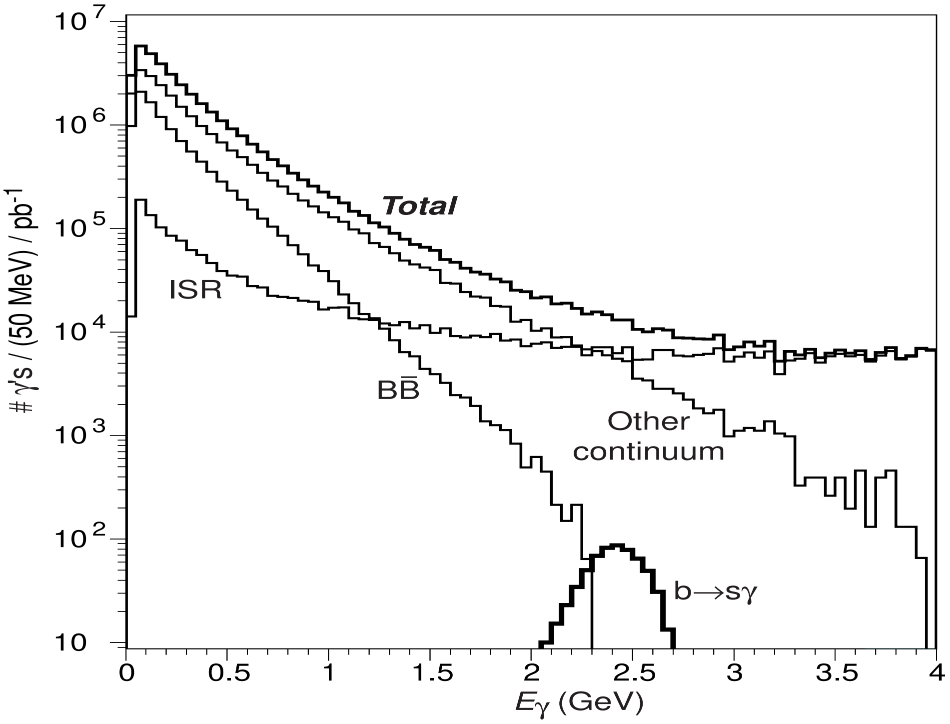

Figure 6: E_γ expected spectrum and its backgrounds (log scale).

The background from continuum annihilation is suppressed by using: (i) a neural net of various shape variables; (ii) "pseudo-reconstruction", i.e. identifying a strange mesonic system (K+up to $4\pi(\leq 1\pi^\circ)$), and combining it with the γ to get acceptable B candidate mass and ΔE and (iii) presence of a high energy lepton (from the other B). Each event is weighted by a combination of the above with weights determined using neural nets trained on Monte Carlo simulation. The continuum background is thus reduced to only about three times the signal and it is then completely removed by subtracting off-resonance data from on-resonance data (fig. 7a).

The background from $B\overline{B}$ is suppressed by vetoing the γ that form a π° or an η. It is then evaluated by a specially tuned Monte Carlo simulation and subtracted.

From a MC simulation using Ali and Greub model we found the efficiency $\epsilon = (4.26 \pm 0.25) \times 10^{-2}$

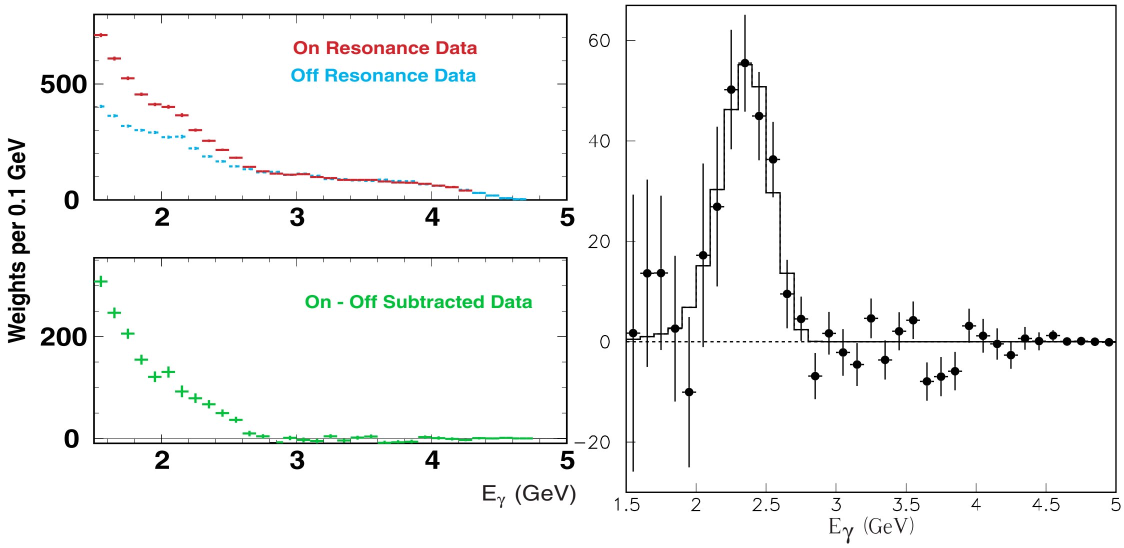

Figure 7: (a) Laboratory E_γ spectrum before and after continuum annihilation subtraction. (b) same spectrum after $B\overline{B}$ background subtraction, with MC simulation superimposed

After adjusting for the spectrum below 2.0 GeV and for the small $b \rightarrow d\gamma$ contamination we find the following branching fraction:

$$\mathcal{B}(b \rightarrow s\gamma) = (3.03 \pm 0.47) \times 10^{-4} \tag{2}$$

consistent with the SM prediction. The error includes the systematic error due to uncertainties in background subtractions, detector simulation and $(b \rightarrow s\gamma)$ modeling.

The γ spectrum is shown in fig. 7b. After correcting for the motion of the B in the lab and for detector resolution, we found (for $E_\gamma > 2.0$ GeV) the following moments:

$$\langle E_\gamma \rangle = 2.346 \pm 0.030 \pm 0.01\ GeV, \tag{3}$$

$$\langle E_\gamma^2 - \langle E_\gamma \rangle^2 \rangle = 0.021 \pm 0.007 \pm 0.002\ GeV^2 \tag{4}$$

These measurements, combined with the moments of the hadronic effective mass squared distribution in the B semileptonic decay $B \to X_c \ell \nu$, lead to an improved extraction of $|V_{cb}|$. Heavy Quark Effective Theory (HQET) and the Operator Product Expansion (OPE) allow to expand these moments, as well as the width Γ_{sl} of the B semileptonic decay, in powers of α_s and $1/M_B$ [9]. Limiting the expansion to cubic terms in $1/M_B$, three parameters appear, $\overline{\Lambda}$, λ_1 and λ_2 for the linear and quadratic terms, plus five paramters for the cubic terms. These parameters are to be determined by experiment (or possibly calculated with lattice QCD). The $1/M_B^3$ parameters are estimated from dimensional considerations to be $\sim (0.5\text{GeV})^3$ and are not important in the following discussion. The parameter λ_2 is determined, from the $D^* - D$ mass difference or the $B^* - B$ mass difference, to be 0.128 GeV^2. The first and second E_γ moments determine, respectively, $\bar{\Lambda}$ and λ_1. The moments of the hadronic mass distribution in $B \to X_s \ell \nu$ determine bands in the λ_1 vs $\bar{\Lambda}$ plot. Fig. 8 shows that the combination of the first moments determines $\overline{\Lambda}$ and λ_1. Here we used the value $\langle M_X^2 - \bar{M}_D^2 \rangle = 0.287 \pm 0.065$ GeV^2, obtained in separate CLEO analysis [10]. The lighter gray bands are theoretical uncertainties and the ellipse is a 1 σ error ellipse. The values obtained are:

$$\bar{\Lambda} = 0.35 \pm 0.07 \pm 0.10 \text{ GeV} , \tag{5}$$

$$\lambda_1 = -0.216 \pm 0.068 \pm 0.077 \text{ GeV}^2 . \tag{6}$$

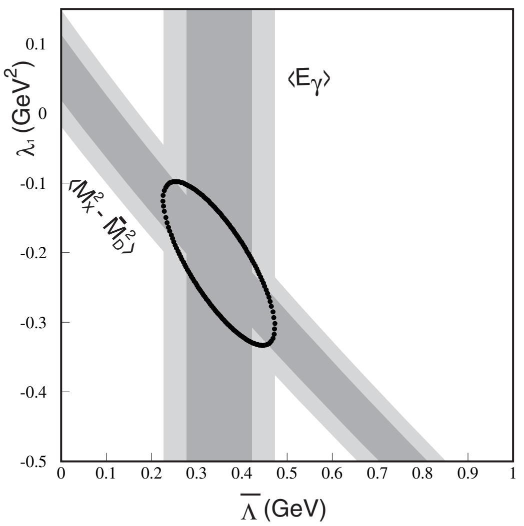

Figure 8: Bands in $\bar{\Lambda} - \lambda_1$ space allowed by our measurements of $\langle E_\gamma \rangle$ and $\langle M_X^2 - \bar{M}_D^2 \rangle$.

We can then use this determination of $\bar{\Lambda}$ and λ_1 and the HQET-OPE expansion of $\Gamma(B \to X_c \ell \nu)$ to improve the determination of $|V_{cb}|$. We use the experimental values $\mathcal{B}(B \to X_c \ell \nu) = (10.39 \pm 0.46)\%$ [CLEO [11]], $\tau_{B^\pm} = (1.548 \pm 0.032) \times 10^{-12}$ sec

[PDG [12]], $\tau_{B^0} = (1.653 \pm 0.028) \times 10^{-12}$ sec [PDG [12]], $f_{+-}/f_{00} = 1.04 \pm 0.08$ [CLEO [13]], gettting $\Gamma_{sl} = (0.427 \pm 0.020) \times 10^{-10}$ MeV. Inserting this value and $\bar{\Lambda}$ and λ_1 given above in the theoretical expression we find:

$$|V_{cb}| = 0.0405 \pm 0.0009 \pm 0.0009 \pm 0.0008 \ , \tag{7}$$

where the errors are from the experimental determination of Γ_{sl}, from the experimental determination of $\bar{\Lambda}$ and λ_1, and from the $1/M_B^3$ terms and scale uncertainty in α_s, in that order.
This gives a determination of $|V_{cb}|$ from inclusive processes, with an accuracy of $\pm 3.7\%$.
The extraction of the value of $|V_{ub}|$ from the measured yield of leptons from $b \to u \ell \nu$ between 2.3 and 2.6 GeV/c [14] needs extrapolating that yield to the full lepton energy range. Several theorists [15] have shown how to use the photon energy spectrum in $b \to s\gamma$ to perform such an extrapolation. Given the great importance of an accurate measurement of $|V_{ub}|$, we plan to use all these methods in conjunction with a new measurement of the $b \to u \ell \nu$ endpoint yield.

6 Limit on CP asymmetry in $B^\circ \overline{B}^\circ \to \ell^\pm \ell^\pm$ [6]

The Standard Model predicts that the mixing rates $B^0 \to \bar{B}^0$ and $\bar{B}^0 \to B^0$ are very nearly equal. Thus, a large CP asymmetry in B°-$\overline{B}^\circ$ mixing would be evidence for New Physics.
In $\Upsilon(4S) \to B^0 \bar{B}^0$ events, where both B mesons undergo semileptonic decay, the "dilepton asymmetry" $a_{\ell\ell}$ is directly related to the real part $\Re(\epsilon_B)$ of the "CP impurity parameter":

$$a_{\ell\ell} \equiv \frac{N(\ell^+\ell^+) - N(\ell^-\ell^-)}{N(\ell^+\ell^+) + N(\ell^-\ell^-)} = \frac{4\Re(\epsilon_B)}{1 + |\epsilon_B|^2} \tag{8}$$

The big problem in this measurement is the large number of correction terms, each one affected by statistical and/or systematic errors, needed to get the *true* $a_{\ell\ell}$ from the measured $a_{\ell\ell}^m$, leading to a large overall systematic error. We have found that a drastic reduction of the systematic error on $a_{\ell\ell}$ is possible when combining the measurement of $a_{\ell\ell}$ with that of the single lepton asymmetry a_ℓ.
Our result [6] is $a_{\ell\ell} = (+0.013 \pm 0.050 \pm 0.005)(1.00 \pm 0.10)$ in good agreement with our recent measurement $a_{CP} = +0.017 \pm 0.070 \pm 0.014$, via partial hadron reconstruction [16]. Dividing by 4 the weighted average of the two, we obtain:

$$\frac{Re(\epsilon_B)}{1 + |\epsilon_B|^2} = +0.0035 \pm 0.0103 \pm 0.0015. \tag{9}$$

This result is consistent with zero and the Standard Model predictions. Although we lack the statistics needed to see any discrepancy with the Standard Model, we found a method that drastically reduces the systematic error.

7 Charm Physics

Mixing and CP violation in D° decay are an excellent hunting grounds in the search for New Physics. That is so because the Standard Model predicts very small mixing amplitudes: ($10^{-6} < |x|,\ |y| < 6 \times 10^{-2}$) and even smaller CP violation asymmetries $\mathcal{O}(10^{-3})$. I'll summarize four recent results:

- Search for Lifetimes difference due to D°-$\overline{D}^\circ$ mixing and the mixing parameter $y_{CP} = \frac{\Delta\Gamma}{2\Gamma}$ [17].
- Limits on CP asymmetries in $D^\circ \to K^+K^-$, $\pi^+\pi^-$, $K^\circ_S\pi^\circ$, $\pi^\circ\pi^\circ$, $K^\circ_S\pi^\circ$ [18].
- First measurement of the rate of wrong-sign $D^0 \to K^+\pi^-\pi^0$ [19].

Futhermore I'll report the first measurement of the long sought, very small decay width of the D^{*+}: $\Gamma(D^{*+})$ [20].
Finally, I'll mention an unexpected correlations betewen Λ_c and $\overline{\Lambda}_c$ in $e^+e^- \to c\overline{c}$ annihilation [21].

8 Search for Lifetimes difference due to D°-$\overline{D}^\circ$ mixing and the mixing parameter $y_{CP} = \frac{\Delta\Gamma}{2\Gamma}$ [17]

Neglecting CP violation, the two D° CP eigenstates, $D_+,\ D_-$ have (slightly) different decay rates: $\Gamma_\pm = \Gamma(1 \pm y_{CP})$ where Γ is the average of them and $y_{CP} = \Delta\Gamma/2\Gamma \ll 1$ is one of the two mixing parameters, under the hypothesis of CP conservation. y_{CP} can thus be obtained from the D° average lifetime $\overline{\tau}$ and the average lifetime τ_+ of the CP=+1 eigenstate,D_+:

$$y_{CP} = 1 - \frac{\overline{\tau}}{\tau_+} \tag{10}$$

From a sample of $20,272 \pm 178$ $D^\circ \to K^-\pi^+$ (and charge conjugate) decay from which we extract $\overline{\tau}$. From $2,463 \pm 65$ $D^\circ \to K^-K^+$ and 930 ± 37 $D^\circ \to \pi^+\pi^-$ we extract τ_+. Fig. 9 shows the effective mass distributions for these three decay modes. The parametrization of the signal is obtained from the first, largest sample of decays to $K^-\pi^+$.

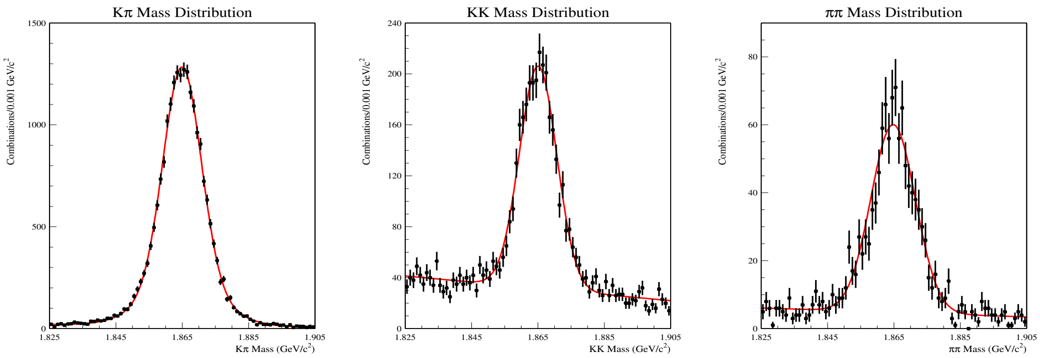

Figure 9: Effective mass distributions for the $K^{\mp}\pi^{\pm}$, K^+K^- and $\pi^+\pi^-$ samples.

An accurate measurement of the D° time of flight is possible because of the vertically narrow luminous region ($\sigma_{vertical} = 7\ \mu$m, centroid resolution less than $5\mu m$), good vertexing (typical error $\sim 40\mu m$) and the use of D°s that are daughters of $D^{*\pm}$. We use only the vertical component of the D° flight distance. The proper liftime distributions are shown, for the three samples, in fig. 10.

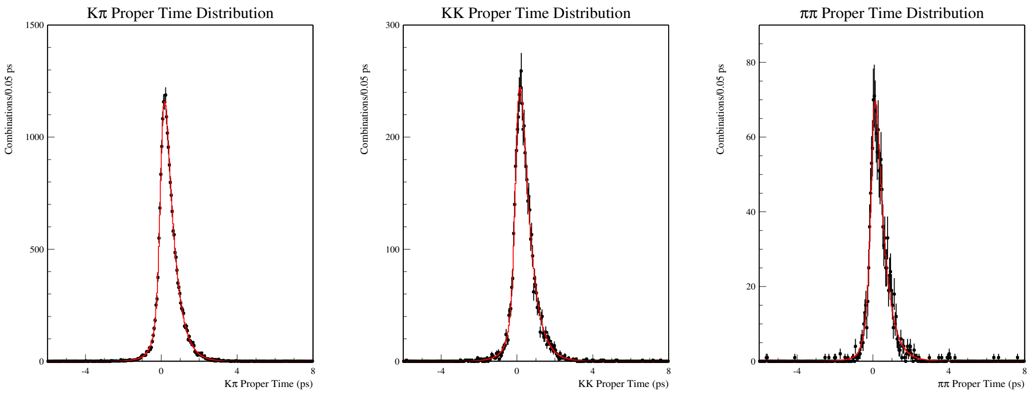

Figure 10: Lifetime distributions for $D^{\circ}\rightarrow K^{\mp}\pi^{\pm}$, for $D^{\circ}\rightarrow K^-\pi^+$ and for $D^{\circ}\rightarrow\pi^+\pi^-$ candidates, respectively.

The measured proper lifetimes are: $\overline{\tau} = 0.4046 \pm 0.0036$ ps for the $K^{\mp}\pi^{\pm}$ sample, $\tau_+ = 0.411 \pm 0.012$ ps for the $K^-\pi^+$ sample and $\tau_+ = 0.401 \pm 0.017$ ps for the $\pi^+\pi^-$ sample. They give: $y_{KK} = -0.019 \pm 0.029 \pm 0.016$ and
$y_{\pi\pi} = +0.005 \pm 0.043 \pm 0.018$.
Taking the weighted average of y_{KK} and $y_{\pi\pi}$ we finally find:

$$y_{CP} = -0.011 \pm 0.025(\text{stat}) \pm 0.014(\text{syst})\ (\text{PRELIMINARY}) \tag{11}$$

consistent with 0 and with previous results from CLEO [22] and FOCUS [23].

9 Limits on CP asymmetries in $D^\circ \to K^+K^-$, $\pi^+\pi^-$ [18]

The asymmetry we want to measure:

$$A = \frac{\Gamma(D^\circ \to f) - \Gamma(\overline{D}^\circ \to f)}{\Gamma(D^\circ \to f) + \Gamma(\overline{D}^\circ \to f)} \tag{12}$$

is obtained tagging the D° flavor from the charge of its parent $D^{*\pm}$. We used the final states $K^+K^-$and $\pi^+\pi^-$. The D° yields are obtained by fitting the $D^{*\pm}$ energy release $Q \equiv M^* - M - m_\pi$ distributions, shown in fig. 11.

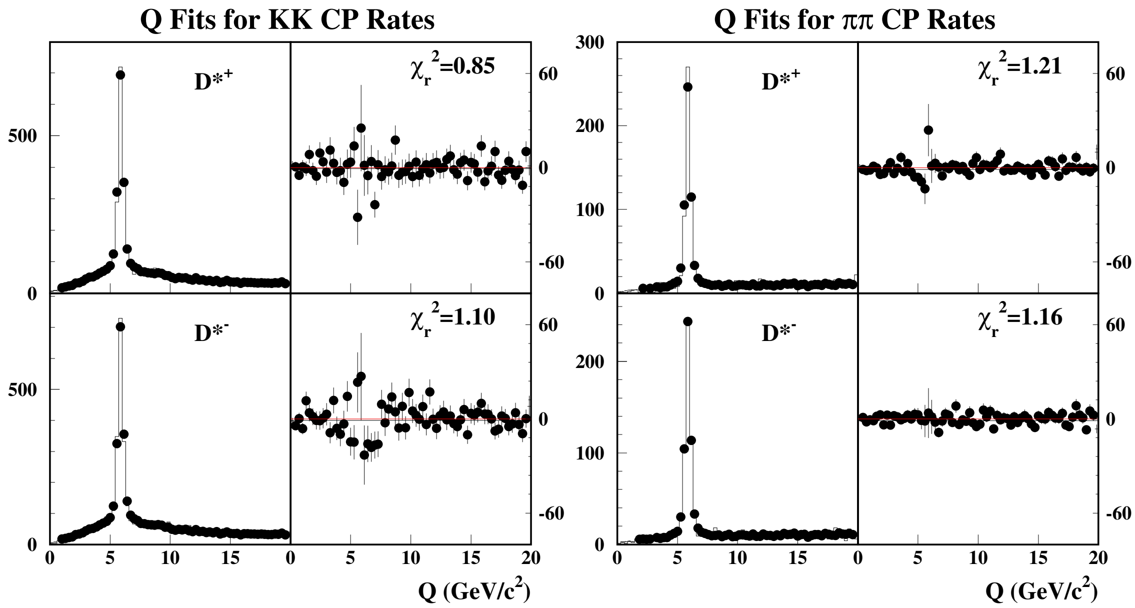

Figure 11: Q distributions for $D^0 \to K^+K^-$ (left) and $D^0 \to \pi^+\pi^-$ (right) candidates separated into samples tagged as D^{*+} (top) and D^{*-} (bottom). Shown immediately to the right of each Q distribution are the point by point residuals of the fit. In each case the data points are shown with error bars and the solid line represents our fitting results.

The preliminary results are:

$$A(K^+K^-) = (0.05 \pm 2.2 \pm 0.8)\% and A(\pi^+\pi^-) = (2.0 \pm 3.22 \pm 0.8)\%. \tag{13}$$

They are consistent with 0: no CP asymmetry is detected.

10 Limits on CP asymmetries in $D^\circ \to K^\circ_S\pi^\circ$, $\pi^\circ\pi^\circ$, $K^\circ_S K^\circ_S$ [18]

The $K^\circ_S K^\circ_S$ case treated very similarly to K^+K^-, $\pi^+\pi^-$ case. In the $K^\circ_S\pi^\circ$ and $\pi^\circ\pi^\circ$ cases, vertex reconstruction is not possible, however the yield of D° and $\overline{D}^\circ$ can be obtained by fitting the $D^{*\pm}$ energy release distributions, as shown in fig. 12.

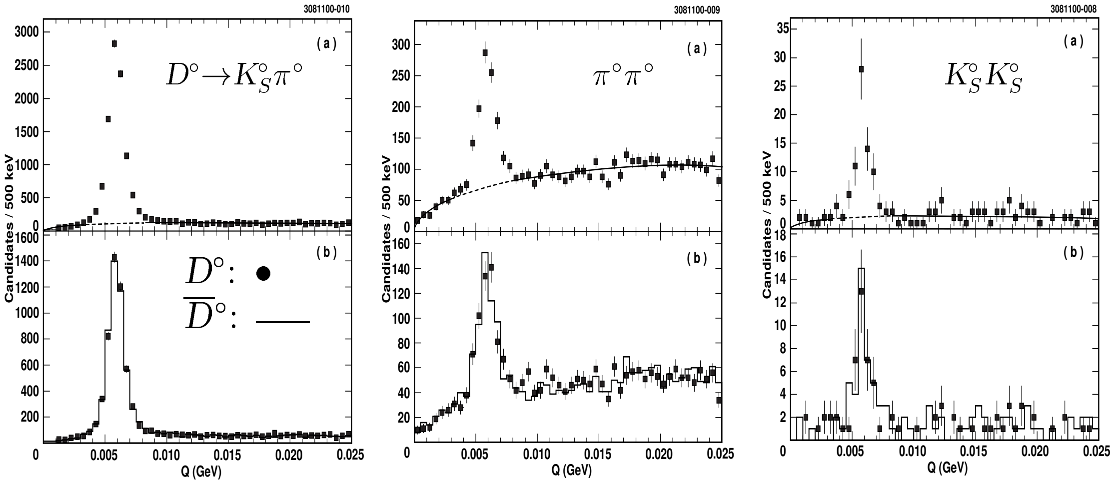

Figure 12: Fitted Q distribution for $D^0 \to K_S^0 \pi^0$, $D^0 \to \pi^0 \pi^0$, $D^0 \to K_S^0 K_S^0$ candidates, respectively. The points with error bars are data; in (a) the solid line represents the background and the dashed line shows the interpolation into the Q signal region; (b) shows the Q distributions for D^0 (points) and for $\overline{D^0}$ (histogram) candidates.

The measured asymmetries are (statistical and systematic errors are combined):
$A(K_S^0 \pi^0) = (+0.1 \pm 1.3)\%$, a significant improvement over previous results;
$A(\pi^0 \pi^0) = (+0.1 \pm 4.8)\%$, and $A(K_S^0 K_S^0) = (-23 \pm 19)\%$ are first measurements.

11 First Observation of Wrong-Sign $D^0 \to K^+ \pi^- \pi^0$ Decay [19]

"Wrong sign" (WS) D° decays may be due to Doubly Cabibbo Suppressed Decays (DCSD) or to mixing. I report on CLEO's first measurement of the "Wrong sign" decay $D^\circ \to K^+ \pi^- \pi^\circ$.
CLEO conducted an extensive study of the rich resonant substructure (ρ^+, K^{*-}, $K^{*\circ}$, ...) of the $D^\circ \to K^- \pi^+ \pi^\circ$ "Right Sign" (RS) decay [24]. It has been suggested [25] that the "Wrong Sign" decay $D^\circ \to K^+ \pi^- \pi^\circ$ may have a different substructure. In principle this may lead to different detection efficiencies for the two cases. We have performed an exhaustive detection efficiency analysis over the Dalitz plot and we found that

$$\frac{\overline{\varepsilon}_{RS}}{\overline{\varepsilon}_{WS}} = 1.00 \pm 0.02 \text{ (stat)}. \tag{14}$$

The ratio of yields was obtained by performing a maximum likelihood fit to the two-dimensional distribution in $m(K\pi\pi)$ vs Q. The projections of the data and fit results on the respective axes are shown in Fig. 13.

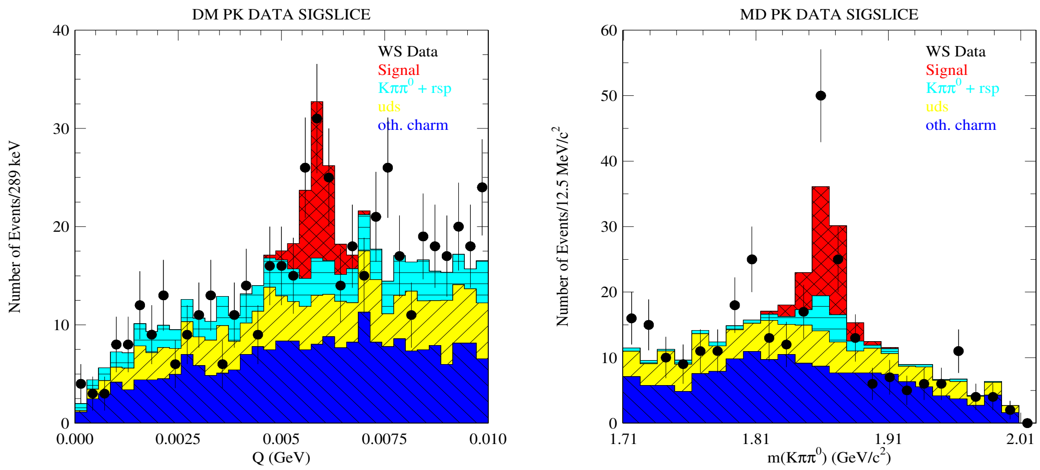

Figure 13: Results of the fit to the data to determine N_{WS}/N_{RS}. Projections on the variable Q (left) and $m(K\pi\pi^0)$ (right), after selecting the signal region in the other variable.

Our preliminary result is:

$$R_{WS} \equiv \frac{\bar{\varepsilon}_{RS}}{\bar{\varepsilon}_{WS}} \cdot \frac{N_{WS}}{N_{RS}} = 0.0043^{+0.0011}_{-0.0010}\,(\text{stat}) \pm 0.0007\,(\text{syst}), \tag{15}$$

consistent with the CLEO II.V [22] and FOCUS [23] $D^0 \to K\pi$ measurements. This measurement of R_{WS} can be used to obtain limits on R_{DCSD} as a function of y' within the limits on x' set by CLEO, as shown in fig. 14. Notice, however, that the variable y' may not be the same for $D^0 \to K^+\pi^-$ and $D^0 \to K^+\pi^-\pi^0$. Work is in progress to use the lifetime distribution of this sample to yield independent limits on x', y', and R_{DCSD}.

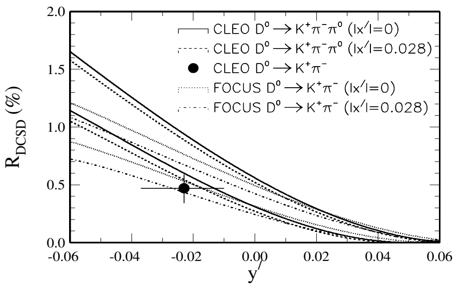

Figure 14: $R_{DCSD}(\%)$ vs y'

12 First measurement of $\Gamma(D^{*+})$

The smallness of the $D^{*\pm}$ radiative branching fraction [26],
$\mathcal{B}(D^{*+} \to D^+\gamma) = (1.68 \pm 0.45)\%$,
tells us that the $D^{*\pm}$ decay probability, $\Gamma(D^{*+})$, is dominated by a strong decay process. Thus a measurement of $\Gamma(D^{*+})$ opens an important window on the

non-perturbative strong physics involving heavy quarks. Theoretical predictions vary widely [27]: $15 < \Gamma(D^{*+}) < 150$ keV.

The only previous measurement [28], based on just 110 events, could only give an upper limit: $\Gamma(D^{*+}) < 131$ keV. Our sample of 13,000 events: $D^{*+} \to \pi^+_{slow} D^0$, $D^0 \to K^- \pi^+$, collected with the CLEO II.V detector (fig. 15) allowed us to produce the first measurement of $\Gamma(D^{*+})$.

The measurement of $\Gamma(D^{*+})$ is made possible by a $D^{*\pm}$ recontruction method that takes advantage of the already mentioned, small vertical size of the CESR beam spot, resulting in very good resolution in the distribution of the energy release in the $D^{*+} \to D^0 \pi^+$ decay.

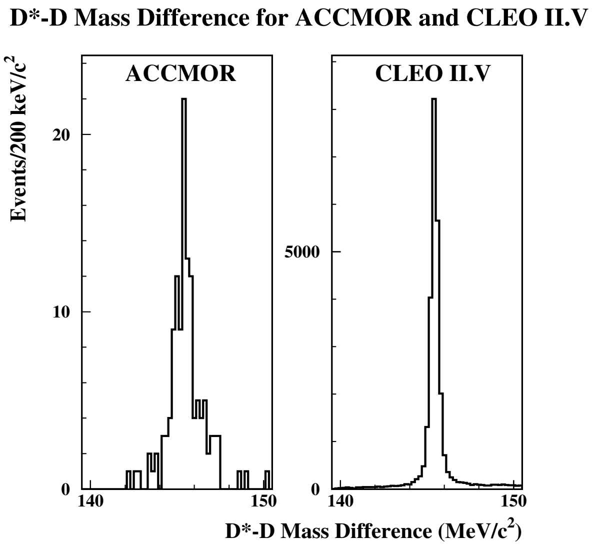

Figure 15: The D^{*+} - D^0 mass difference distribution obtained by ACCMOR (left) and in this work (right).

Our procedure is based on fitting this energy release, $Q \equiv M(K^- \pi^+ \pi^+_{slow}) - M(K^- \pi^+) - M(\pi^+)$ with the convolution of a Breit-Wigner and a Gaussian distribution due to tracking resolution (plus a very small background).

The challenge of this analysis is to understand and minimize tracking errors. We have to take into account *tracking mishaps*, i.e. tracks with mismeasured hits, errors in pattern recognition, kinks due to nuclear collisions and large angle Coloumb scattering. We take them into account by adding a second, wider Gaussian to the fitting function. An additional difficulty is that there is no physical calibration for this measurement so that we must use, and check in a variety of ways, the Monte Carlo simulation of detector.

We started with a raw sample of 13,337 events, that uses standard track selection criteria and D° and $D^{*\pm}$ vertex fitting that exploitsthe vertical narrowness of the luminous beam ribbon by discarding D° within 0.3 radians of horizontal plane. We then added more selections to obtain the following three samples.

The **Nominal sample** of 11,496 events, has additional selections on $p(\pi_{slow})$ and $D^{*\pm}$ decay opening angle θ vs $p(D^{*+})$, and requires $\sigma_Q < 200$ keV.

The **Kinematic Selected Sample**, of 3,284 events, selects events with most

favorable kinematic configuration, *i.e.* $\left|\frac{\partial Q}{\partial P_{D^0}}\right| \leq 0.005$, $\left|\frac{\partial Q}{\partial P_{\pi_{slow}}}\right| \leq 0.05$..
Finally, the **Tracking Selected Sample**, of 368 events, imposes much stricter cuts on the tracking parameters: (i) requires hits in both $r\phi$ and z views in every layer of the Silicon Vertex Detector (SVX); (ii) the D^0 daughter tracks are required to have at least 38/51 main drift chamber hits and (iii) tracks must have χ^2/DoF<2 in the Drift Chamber and χ^2/DoF<50 in SVX.
A detailed Monte Carlo simulation study showed that the MC with $\Gamma = 90$ keV and DATA are in excellent agreement for the dependence of σ_Q on θ, $p(\pi_{slow})$, $p(D^\circ)$, $\frac{\partial Q}{\partial \theta}$, $\frac{\partial Q}{\partial P_{\pi_{\mathrm{slow}}}}$, and $\frac{\partial Q}{\partial P_{D^0}}$. The agreement is not as good for the dependence of Q itself on these quantities.
We performed an unbinned maximum likelihood fits of the Q distribution of the three selected samples with: (i) a Breit Wigner with a P-wave Γ convoluted with ther esolution Gaussian (width σ_Q), (ii) a small polynomial background, and (iii) (only for Nominal Sample) a Gaussian (width σ_{mis}) to account for *tracking mishaps*.

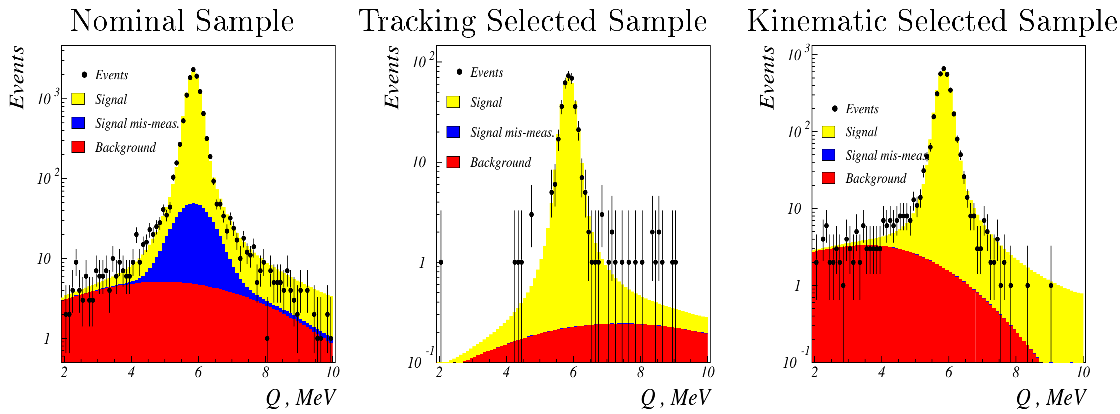

Figure 16: Fits to the three selected data sample. The different contributions to the fit are shown by different colors.

Additional parameters were used for testing and for estimating systematic errors. The fitting procedures for all three samples were tested on large Monte Carlo full simulations generated with $0 < \Gamma(D^{*+}) < 130$ keV. The offsets between the generated and measured values of Q in the three samples are consistent with zero. The fits of the three samples are in excellent agreement:
Nominal sample: $\Gamma(D^{*+}) = 96.2 \pm 4.0$ keV,
Kinematic sample: $\Gamma(D^{*+}) = 103.8 \pm 5.9$ keV,
Tracking sample: $\Gamma(D^{*+}) = 104 \pm 20$ keV.

The systematic uncertainties are, in decreasing order of importance: (i) dependence of Q on the kinematic parameters, (ii) mis-modeling of σ_Q's dependence on the kinematic parameters, (iii) correlations among fit parameters, (iv) small distortion in D° vertex reconstruction, (v) background shape, (vi) uncertainty in offset correction. A dominant source of uncertainty on Q_0 is the energy scale of our measurements: it is still being evaluated.
Since the systematic errors is essentially the same in the three samples, we choose as overall result the one from the Nominal Sample that gives the smallest statistical error:

$$\Gamma(D^{*+}) = 96 \pm 4 \pm 22 \text{ keV}. \tag{16}$$

13 $\Lambda_c\overline{\Lambda}_c$ correlations in $e^+e^- \to c\overline{c}$ [21]

In $e^+e^- \to c\overline{c}$ annihilation, at sufficiently high energy, one expects that the kind of anti-charm hadron produced in the $\overline{c}$ jet be largely independent of what kind of charm hadron is produced in the c jet. Furthermore, when baryons are produced, we expect *and generally see* that baryon and anti-baryon are close in rapidity.
We found that the above is not true in Λ_c production in $e^+e^- \to c\overline{c}$ annihilation. What we found is that the probability of producing a $\overline{\Lambda}_c^-$ in the $\overline{c}$ jet when we have a Λ_c^+ in the c jet is three and a half time the probability of producing a $\overline{\Lambda}_c^-$ in the $\overline{c}$ jet when we have a D in the c jet. In formulae, with hopefully obviuos notation:

$$f_{\overline{\Lambda}_c^-}(c{\to}\Lambda_c^+) = 3.5 \times f_{\overline{D}}(c{\to}\Lambda_c^+). \tag{17}$$

No such correlation was found in events that contained an additional proton: the effect is not due to production of two baryon-antibaryon pairs. We looked for correlations between the different charge states of D vs $\overline{D}$: none was found, as expected.
The quantity we actually measured is the **Ratio of Production Ratios** defined as follows:

$$\frac{\Lambda_c^+|\overline{\Lambda}_c{}^-}{\overline{\Lambda}_c{}^-} \div \frac{\Lambda_c^+|\overline{D^0}}{\overline{D^0}} \tag{18}$$

where the symbols stands for the respective particle yields and the vertical bars in the numerators mean that the charm and anti-charm hadron are at more than 90^o from each other. This ratio of ratios eliminates most of the systematic errors.
This analysis used six Λ_c decay modes: $pK^-\pi^+$, pK_s^0, $\Lambda\pi^+$, $\Lambda\pi^+\pi^-\pi^+$, $pK_s^0\pi^+\pi^-$, and $\Lambda + X$. The selected charm hadrons were required to have momentum $p > 2.3$ GeV in order to exclude products of B decay.

Our result is:

$$\frac{\Lambda_c^+|\Lambda_c^-}{\Lambda_c^-} \div \frac{\Lambda_c^+|\overline{D^0}}{\overline{D^0}} = 3.5 \pm 0.6 \pm 0.4 \tag{19}$$

The systematic errors that do not cancel in ratios are: (i) 6% from the signal shape parametrization and the definition of "signal" and "side" bands, (ii) 5% from differences in different fitting methods and (iii) 7% from variation of the minimum momentum cut.

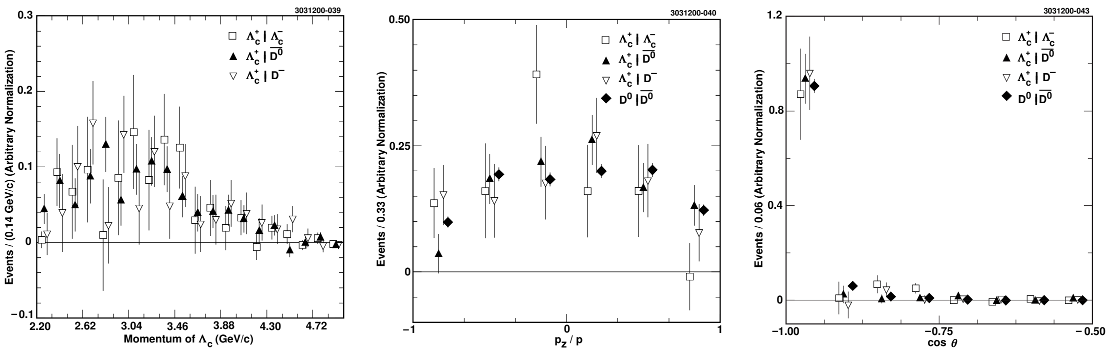

Figure 17: (a) the momentum distribution of the $\Lambda_c$associated with $\overline{\Lambda_c^-}$or $\overline{D}$; (b) similarly for the cosine of the angle between the Λ_c and the beam line; (c) the cosine of the angle between the Λ_c and different anticharm hadrons.

It is important to note that the Λ_c momentum distribution and its angular correlations with the beam and with the anti-charm hadron in the $\overline{c}$ jet (see fig. 17) are as expected for the jet's leading hadron and independent of the kind of anti-charm hadron in the $\overline{c}$ side of the event.
We did not see in JETSET any mechanism to generate this kind of correlation.

14 The new CLEO results I had to omit

- A Search for Charmless $B \to VV$ Decays [hep-ex/0101029]
- Bounds on the CP Asymmetry in $b \to s\gamma$ Decays [hep-ex/0010075]
- Study of $B \to \psi(2S)K$ and $B \to \psi(2S)K^*(892)$ Decays, Phys.Rev. **D63** (2001) 031103 [hep-ex/0010036]
- Study of χ_{c1} and χ_{c2} Meson Production in B Meson Decays: Phys.Rev. **D63** (2001) 031102 [hep-ex/0009044]

- First Observation of the Decays $B^0 \to D^{*-} p\bar{p}\pi^+$ and $B^0 \to D^{*-} p\bar{n}$ [hep-ex/0009011]
- Dalitz Analysis of the Decay $D^0 \to K^-\pi^+\pi^0$ [hep-ex/0011065]
- Observation of the Ω_c^0 Charmed Baryon at CLEO [hep-ex/0010035]
- Evidence of New States Decaying into $\Xi_c'\pi$ [hep-ex/0012020]
- Search for Direct CP Violation in Ξ Hyperon Decay [hep-ex/0009037]
- A Measurement of the Decay Asymmetry Parameters in $\Xi_c^0 \to \Xi^-\pi^+$ [hep-ex/0011073]
- Measurement of the Λ_c^+ Lifetime [hep-ex/0011049]
- Observation of New States Decaying into $\Lambda_c^+\pi^-\pi^+$ [hep-ex/0010080]
- Study of τ Decays to Six Pions and Neutrino [hep-ex/0010025]

15 Acknowledgements

The CLEO Collaboration gratefully acknowledges the effort of the CESR staff in providing us with excellent luminosity and running conditions. This work was supported by the National Science Foundation, the U.S. Department of Energy, the Research Corporation, the Natural Sciences and Engineering Research Council of Canada, the Swiss National Science Foundation, the Texas Advanced Research Program, and the Alexander von Humboldt Stiftung.

References

1. CLEO Collaboration, Y. Kubota *et al.*, Nucl. Instrum. Methods Phys. Res., Sect. A **320**, 66 (1992).
2. CLEO Collaboration, T. Hill *et al.*, Nucl. Instrum. Methods Phys. Res., Sect. A **418**, 32 (1998).
3. CLEO Collaboration, R.A. Briere *et al.*, hep-ex/0101032
4. CLEO Collaboration, D.M. Asner *et al.*, hep-ex/0103040
5. CLEO Collaboration, T. E. Coan, *et al.*, hep-ex/0010075

6. CLEO Collaboration, D.E. Jaffe *et al.*, CLNS 01/1717, hep-ex/0101006

7. N. G. Deshpande and J. Trampetic, Phys. Rev. D **41**, 895 (1990); L.-L. Chau *et al.*, Phys. Rev. D **43**, 2176 (1991); A. Deandrea *et al.*, Phys. Lett. B **318**, 549 (1993); A. Deandrea *et al.*, Phys. Lett. B **320**, 170 (1994); A.J. Davies, T. Hayashi, M. Matsuda, and M. Tanimoto, Phys. Rev. D **49**, 5882 (1994); G. Kramer, W. F. Palmer, and H. Simma, Nucl. Phys. B **428**, 429 (1994); G. Kramer, W. F. Palmer, and H. Simma, Zeit. Phys. C **66**, 429 (1995); D. Du and L. Guo, Zeit. Phys. C **75**, 9 (1997).

8. M. Gronau and D. London, Phys. Rev. Lett. **65**, 3381 (1990)

9. A. F. Falk, M. Luke, and M. J. Savage, *Phys. Rev.* D **53**, 2491 (1996); *Phys. Rev.* D **53**, 6316 (1996); Adam Falk and Michael Luke, *Phys. Rev.* D **57**, 1 (1998).

10. CLEO Collaboration, to be published.

11. B. Barish *et al.* (CLEO), *Phys. Rev. Lett.* **76**, 1570 (1996).

12. D. E. Groom *et al.* (PDG), *Eur. Phys. J.* **C15**, 1 (2000).

13. J. P. Alexander *et al.* (CLEO), hep-ex/0006002.

14. J. Bartelt *et al.* (CLEO) *Phys. Rev. Lett.* **71**, 4111 (1993).

15. Matthias Neubert, *Phys. Rev.* D **49**, 4623 (1994); A. K. Leibovich, I. Low, and I. Z. Rothstein, *Phys. Rev.* D **61**, 053006 (2000); A. L. Kagan and M. Neubert, *Eur. Phys. J.* **C7**, 5 (1999).

16. CLEO Collaboration, B.H. Behrens *et al.*, Phis. Lett. **B490**, 36 (2000).

17. CLEO Collaboration, D. Cronin-Hennesy *et al.*, hep-ex/0102006.

18. CLEO Collaboration, G. Bonvicini *et al.*, Phys.Rev. **D63** (2001) 071101, hep-ex/0012054.

19. CLEO Collaboration, D. Cronin-Hennesy *et al.*, hep-ex/0102006.

20. CLEO Collaboration, T.E. Coan *et al.*, hep-ex/0102007.

21. CLEO Collaboration, A. Bornheim *et al.*, hep-ex/0101051.

22. CLEO Collaboration, R. Godang *et al.*, Phys. Rev. Lett. **84**, 5038 (2000).

23. FOCUS Collaboration, J.M. Link *et al.*, hep-ex/0012048, Phys. Lett. **B485**, 62 (2000).

24. CLEO Collaboration, S. Kopp *et al.*, Phys.Rev. **D63** (2001) 092001, hep-ex/0011065.

25. M. Gronau, J. L. Rosner, hep-ph/0010237, to be published in Phys. Lett. B.

26. J. Bartelt *et al.* (CLEO Collaboration), Phys. Rev. Lett. **80**, 3919, (1998).

27. R. Ruckl, WUE-ITP-98-011, CERN-TH/98-124, hep-ph/9810338 is a recent survey summarizing and referencing previous theoretical work. P. Singer hep-ph/9910558, and J. L. Goity and W. Roberts JLAB-THY-00-45, hep-ph/0012314 appeared since that survey.

28. S. Barlag *et al.*, Phys. Lett. **B 38**, 480 (1992).